corner rods. The gap and the filling-component radius can be varied to reduce the temperature nonuniformity very considerably, which should be borne in mind in choosing these components and the jacket dimensions.

NOTATION

u, velocity; μ, dynamic viscosity; ε, turbulent viscosity; ν, kinematic viscosity; ρ, density; c_p, specific heat; D, diffusion coefficient; q_V, volume heat production; q_l, linear heat flux; λ, thermal conductivity; m, molecular mass; Q_r, heat of reaction; z, longitudinal coordinate. Subscripts: I and II, reactions $N_2O_4 = 2NO_2$ and $2NO_2 = 2NO + O_2$ correspondingly; 1) N_2O_4; 2) NO_2; 3) NO; 4) O_2; fu, fuel; c, cladding; f, frozen value; w, wall.

LITERATURE CITED

1. V. B. Nesterenko and B. E. Tverkovkin, Heat Transfer in a Nuclear Reactor Containing a Dissociating Coolant [in Russian], Minsk (1980).
2. A. P. Yakushev, B. E. Tverkovkin, V. B. Nesterenko, and I. G. Nemtseva, Vestsi AN BSSR, Ser. Fiz.-Energ. Nauk, No. 4, 124-128 (1975).
3. V. B. Nesterenko, B. E. Tverkovkin, A. P. Yakushev, and T. I. Mikryukova, Vestsi AN BSSR, Ser. Fiz.-Energ. Nauk, No. 4, 102-106 (1976).
4. N. I. Buleev, Wall Turbulent Flow [in Russian], Part 1, Novosibirsk (1975), pp. 51-79.
5. T. V. Besedina, A. V. Udot, and A. P. Yakushev, Problems at Nuclear Power Stations with Dissociating Coolants [in Russian], Minsk (1985), pp. 111-117.
6. G. Declout, The Finite-Element Method [Russian translation], Moscow (1976).

NUMERICAL MODELING OF MOTION OF AN AXISYMMETRIC BODY THROUGH A TUNNEL

O. G. Goman, V. I. Karplyuk, and M. I. Nisht

UDC 532.5

The method of discrete vortices is used for a numerical investigation of the nonlinear unsteady problem of passage of an axisymmetric body through a coaxial thin-walled cylindrical tube of finite length.

Because of the increased speed of trains and the development of tube-borne transport and other areas of technology it is becoming increasingly important to study the interaction of moving bodies and the solid boundaries surrounding them.

The first approximate schemes for calculating the drag of a train moving within a tunnel were proposed at the end of the thirties and were based mainly on experimental data. For instance, in [1] a semiempirical method was developed of calculating the drag of a train on an open track and in a long tunnel (the tunnel was considered long if we can neglect the unsteady effects due to its ends).

At present quite a wide circle of topics in the aerodynamics of fast trains has been investigated [2]. However, nonlinear problems have been examined only for steady motion [3, 4], and [4] presented the results of calculated steady flow of an infinite chain of containers on the basis of numerical solution of the full Navier–Stokes and Reynolds equations.

Unsteady problems of the aerodynamic effect of a tunnel on a train have been investigated only approximately, in linear formulation, within the framework of planar and other models [5-8]. However, for short tunnels, the unsteady effects due to the entrance of the

Translated from Inzhenerno-Fizicheskii Zhurnal, Vol. 54, No. 2, pp. 216-221, February, 1988. Original article submitted October 30, 1986.

0022-0841/88/5402-0148$12.50

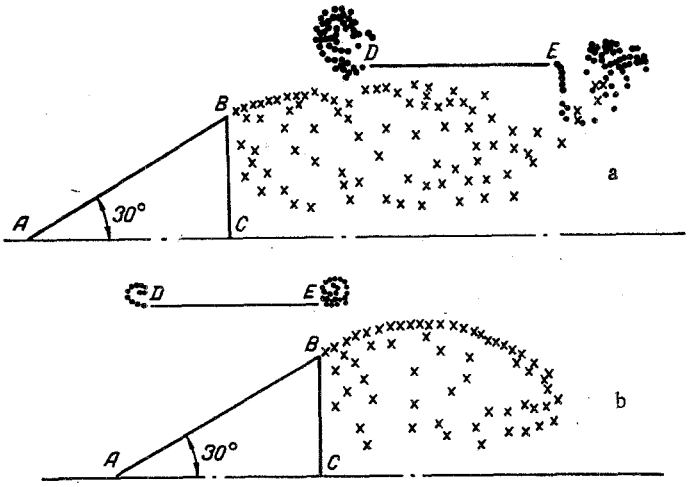

Fig. 1. Shape of a vortex sheet and position of the cone relative to the tunnel at time $\tau = 60/23$ (b) and $\tau = 90/23$ (a).

train into the tunnel and its exit from the tunnel play an important role, and they are nonlinear, since they are due to flow separation in the entrance and exit tunnel sections.

The present paper gives a numerical solution of the problem of passage of an axisymmetric body through a short tunnel in the form of a thin-walled tube coaxial with the moving body. All three phases of motion of the body through the tunnel have been investigated: the entrance process, the inside motion, and exit from the tunnel. At each time step we determined the pressure distribution over the body surface and on the internal walls of the tunnel and the drag coefficient of the moving body. (The drag force coefficient obtained is only part of the total drag, since the friction force is not taken into account.)

As an example we consider a sharp cone with a semivertex angle of $\theta_k = 30°$ and a flat base, beginning to move impulsively from rest with constant speed U from an initial position at distance S_0 from the tunnel entrance equal to the diameter of the cone base.

It is postulated that in the process of motion axisymmetric vortex sheets are shed from the sharp edges of the cone and also from the entrance and exit ends of the tunnel, and that for the tunnel the vortices leave tangentially to the generators, and for the cone tangentially to the side surface.

The problem was solved by the method of discrete vortices [9], according to which the surface of the conical body, the cylindrical tube, and the vortex sheets were modeled by a finite system of ring vortices. The boundary conditions of impermeability were fulfilled at control points located midway between the discrete vortices. To fulfill the Chaplygin–Zhukov hypothesis at the sharp edges (places of release of the vortex sheets) the control points were located directly at the sharp edges, and the nearest free vortices were on tangents to the surface of the modeled body along the direction of release of the sheets. To make rational use of machine time on the side surface of the cone we used a nonuniform scheme of subdivision into discrete vortices and control points, and a uniform scheme on the surface of the cone base and on the tube.

For a number of control points equal to m the surfaces of the body and the tunnel were modeled by a system of $m - 3$ ring vortices. The system of equations to determine the circulations of the $m - 3$ bound and the three free vortices shed into the flow at the computing time τ from the sharp edges was adopted in the form

$$\sum_{\mu=1}^{m} \Gamma_{\mu\nu} [v_{\mu x} \cos(n, x) + v_{\mu r} \cos(n, r)] + W_0 = 2\pi \cos(\mathbf{U}, \mathbf{n}) - \\ - \sum_{i=1}^{3} \sum_{s=m+1}^{m+\tau-1} \Gamma_{sv}^{i} [v_{sx}^{i} \cos(n, x) + v_{sr}^{i} \cos(n, r)], \quad \nu = 1, 2, \ldots, m. \tag{1}$$

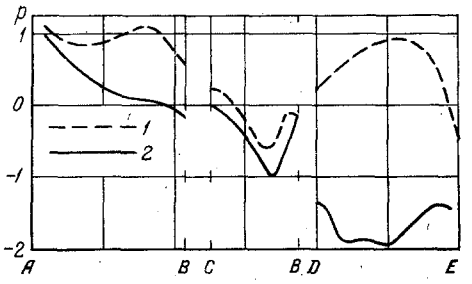

Fig. 2

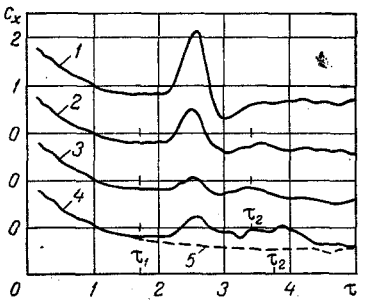

Fig. 3

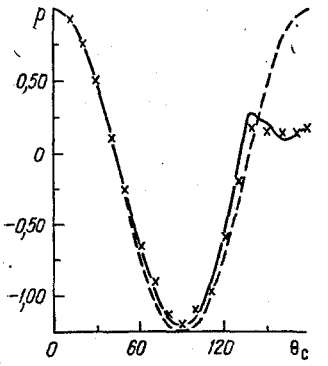

Fig. 4

Fig. 2. Distribution of pressure coefficient over the surface of the cone and the inside wall of the tunnel [1) τ = 60/23; 2) 90/23; L_t = 0.8; R_t = 0.7].

Fig. 3. The cone drag coefficient c_x as a function of time for tunnels of different radii and lengths: 1) L_t = 0.8; R_t = 0.55; 2) 0.8 and 0.6; 3) 0.8 and 0.7; 4) 1.2 and 0.7; 5) $R_t = \infty$ (τ_1 is the time of entrance, and τ_2 is the time of exit of the cone from the tunnel).

Fig. 4. Comparison of the calculated and experimental values of the pressure coefficient on a sphere.

All the quantities in the calculations were used in dimensionless form. As the scales we chose: for length, the cone diameter D; for the calculations, UD; for the induced velocities, U; for time, D/U; for pressure, the velocity head $\rho_\infty \frac{U^2}{2}$.

The system of equations (1) was supplemented by the condition of conservation of circulation around a closed contour passing through the tube and spanning the vortex sheets shed from its ends:

$$\sum_{\mu=k+2}^{m} \Gamma_{\mu\, m+1} + \sum_{i=2}^{3} \sum_{s=m+1}^{m+\tau-1} \Gamma^i_{s\, m+1} = C. \qquad (2)$$

Here k is the number of bound discrete vortices, modeling the contour surface; and C is a constant determined from the initial conditions. If at the initial time τ = 0 the surrounding fluid is at rest, then C = 0.

The formulas for the velocities induced by the ring vortices were taken from [9], the potential of the velocities was found by integrating the velocity field [10], and the pressure coefficient on the surface of the cone and the tunnel was found from the Cauchy–Laplace integral. From the pressure distribution obtained at each time step we determined the drag force coefficient of the cone.

A series of calculations was made for tunnels of different lengths (L_t = 0.8, 1.2) and radii (R_t = 0.55, 0.6, 0.7), and for a cone moving in an unbounded fluid $R_t = \infty$. Some results of the calculations are shown in Figs. 1-3.

It was observed that the mutual influence of the cone and the tunnel begins only from the time when the distance between them becomes less than 0.4, and appears as an increase of pressure on the internal tunnel walls and the side surface of the cone. Up to the time when the cone nose enters the tunnel the latter has in fact no significant influence on the structure and the intensity of the cone vortex sheet and on the intensity of the vortex sheets shed from the ends of the tunnel.

At time $\tau = 50/23$ the cone nose reaches the middle of the tunnel. On the part of the side surface of the cone that has entered the tunnel we note an increase of pressure coefficient. The same thing is observed on the inner surface of the tunnel. And on the side surface of the cone and on the inside of the tunnel the increase of pressure coefficient is directly proportional to the length and inversely proportional to the tunnel radius. Because of the increase of pressure coefficient on the side surface of the cone this time is characterized as the start of a sharp increase of the cone drag coefficient (Fig. 3).

The most characteristic time is $\tau = 60/23$ when the entire cone enters the tunnel (Fig. 1). At this time the vortices shed from the entrance end of the tunnel have maximum intensity and begin to be swirled by the strong flow of fluid leaving the side surface of the cone, in a counterclockwise spiral. The vortex sheet shed from the exit end of the tunnel is also swirled in a spiral, but clockwise, and its vortices do not attain the maximum intensity.

At time $\tau = 60/23$, because of the considerable blocking of the section between the cone and the tunnel, there is a sharp increase of pressure on the side surface of the cone and the tunnel walls. The distribution of pressure coefficient over the surface of the cone and the tunnel has the form of a hump whose apex is ahead of the sharp edge of the cone. Directly at the sharp edge of the cone and on the surface of the tunnel opposite the edge of the cone the pressure coefficient falls because of the large tangential velocities (Fig. 2).

At this time the drag coefficient c_x of the cone reaches a maximum (Fig. 3), and here the value of the peak of the c_x coefficient is greater, the smaller is the tunnel radius, and it can be several times greater than the value of c_x for a cone moving according to the same law in a boundless fluid.

Upon further passage of the cone into the tunnel we observe the very interesting phenomenon accompanied by a sharp fall of the cone drag coefficient (Fig. 3). This occurs in the time interval $\tau = 60/23$-$70/23$, and the narrower is the tunnel, the greater is this fall. For the tunnel with $R_t = 0.55$ the minimum value of c_x is roughly a factor of two less than is c_x of a cone in a boundless fluid. A sharp fall of cone drag is observed at the moment when the cone nose exits from the tunnel, and is a consequence of both the reduction of pressure on the side surface, and of the increase of base pressure due to outflow of fluid into the base region via the slit between the middle of the body and the tunnel wall.

As the cone moves towards the exit section the pressure coefficient on the inside tunnel walls changes from positive to negative.

Immediately after the body exits from the tunnel ($\tau = 80/23$) the base pressure decreases, and this phenomenon leads to the appearance of a second maximum of the pressure coefficient (Fig. 3).

As the distance of the body from the tunnel increases the intensity of the vortices shed from the ends of the tunnel drops, the vortex sheets are broken up and drawn into the rarefaction region inside the tunnel (see Fig. 1). The vortex sheet shed from the sharp edge of the cone is drawn along the axis of symmetry and broken up into two parts (the breakup occurs opposite the exit end of the tunnel). One part, located close to the base rim, is deflected out of the tunnel by the cone, and the other part, located inside the tunnel, is mixed with the vortices shed from the ends, and remains inside the tunnel.

The distribution of pressure coefficient over the side surface of the cone is now independent of the tunnel radius and coincides with the value for a cone moving in a boundless fluid according to the same law as for transit of the tunnel. The distribution of pressure coefficient over the base is also close to that for the case of motion in a boundless fluid, although at time $\tau = 90/23$ the influence of the tunnel is still perceived (Fig. 2).

After the cone has moved away from the exit section a distance on the order of a caliber the influence of the tunnel on the cone ceases, but in the tunnel itself a pressure oscillation at the walls is observed for a long time, due to the vortices remaining there.

The authors know of no experimental data corresponding to the problem examined, with which they could compare, to assess the closeness of the calculated characteristics to the real flow picture, and therefore, in order to check the validity of the method they calculated separated and unseparated flow over a sphere. The broken curve on Fig. 4 corresponds to the model of unseparated flow over a sphere, and hardly differs (with an error of less than 1%) from the theoretical curve $p=1-\frac{9}{4}\sin^2\theta_c$. The solid curve corresponds to separated flow over a sphere with a fixed separation location at $\theta_c = 140°$. The points indicate the experimental results for separated flow over a sphere in the supercritical regime, taken from [11]. From the latter data one can conclude that the computed results for passage of the body through the tunnel will satisfactorily describe the actual flow picture at Reynolds numbers for which a developed vortex wake is found behind the body.

NOTATION

U, velocity of the body; Γ_μ, Γ_s^i, circulation of the bound and free ring vortices; $v_{\mu x}$, $v_{\mu r}$, v_{sx}^i, v_{sr}^i, components of the velocities of the ring vortices; x, r, axes of a cylindrical coordinate system; m, number of control points on the body surface and the tunnel; n, normal to the surface; cos(n, x), cos(n, r), cosines of the angles between the surface normal and the coordinate axes; W_0, unknown value for regularization; τ, time; R_t, L_t, tunnel radius and length; c_x, drag coefficient of the moving body; p, pressure coefficient; θ_k, half angle at the cone vertex; S_0, distance between the forward edge of the tunnel and the cone nose; θ_c, polar coordinate of points on the surface of a sphere.

LITERATURE CITED

1. G. N. Abramovich, "Calculation of the air drag of a train on an open track and in a tunnel," Trudy Tsentr. Aero. Gidro. Inst., No. 400 (1939).
2. M. I. Gurevich, Trudy MIIT, No. 311, 3-9 (1970).
3. G. I. Vernikov, Trudy VNII Vagonostroeniya, No. 37, 3-11 (1979).
4. A. S. Ginerskii (ed.), Introduction to the Aerodynamics of a Container Transport Tube [in Russian], Moscow (1986).
5. T. Khara, M. Kavachiti, G. Fukuchi, and A. Yamamoto, Monthly Bulletin of the Intern. Assoc. of Railway Congresses, No. 2, 55-74 (1969), Moscow (1969).
6. A. A. Yakushev, Trudy MIIT, No. 343, 118-122 (1971).
7. A. G. Terent'ev, and A. Khakimov, Jet and Cavitation Flow and Contemporary Control Topics [in Russian], Cheboksary (1978), pp. 122-134.
8. A. Khakimov, Dynamics of a Continuous Medium with Subdivision Boundaries [in Russian], Cheboksary (1982), pp. 138-143.
9. S. M. Belotserkovskii and M. I. Nisht, Separated and Unseparated Flow of a Perfect Fluid over Thin Wings [in Russian], Moscow (1978).
10. O. G. Goman and V. I. Karplyuk, Mathematical Methods in the Mechanics of Liquids and Gases [in Russian], Dnepropetrovsk (1984), pp. 65-70.
11. A. K. Martynov, Experimental Aerodynamics [in Russian], Moscow (1958).